European Journal of Neuroscience, Vol. 26, pp. 3113–3125, 2007 doi:10.1111/j.1460-9568.2007.05931.x

Retina expresses a novel variant of the ryanodine receptor

Varda Shoshan-Barmatz,[1] Miri Zakar,[1] Fania Shmuelivich,[1] Edna Nahon[1] and Noga Vardi[2]
[1]Department of Life Sciences, Ben Gurion University of the Negev, Beer Sheva, 84105, Israel
[2]Department of Neuroscience, University of Pennsylvania, Philadelphia, PA, USA

Keywords: calcium pump, photoreceptors, retina, ryanodine receptor

Abstract

Calcium released from intracellular stores via the ryanodine receptor (RyR) mediates a variety of signalling processes. We previously showed that retina expresses the three known types of RyR, but retinal membrane preparations exhibit unique characteristics such as Ca^{2+}-independent [^{3}H]ryanodine-binding and inhibition by caffeine. We have heretofore suggested that the major retinal RyR isoform is novel. The present study aimed to identify this receptor isoform and to localize RyR in mammalian retina. Immunoblotting with specific and pan-antibodies showed that the major retinal RyR has a mobility similar to that of RyR2 or RyR3. Real-time PCR revealed that the major type is RyR2, and RT-PCR followed by sequencing showed a transcript that encodes a protein with ~ 99% identity to RyR2, yet lacking two regions of seven and 12 amino acids and including an additional insertion of eight amino acids. An antibody against RyR2 localized this type to somas and primary dendrites of most retinal neurons. An antibody against RyR1 localized RyR to most somas but also revealed staining in photoreceptor outer segments, concentrated on the disk membranes at their rim. The ryanodine-binding properties and the electrophoretic mobility of RyR from the outer segments were similar to those of the whole retinal preparation. The results thus identify a novel variant of RyR2 which can contribute to regulating photoreceptor Ca^{2+} concentrations. The restricted localization of the outer segment RyR to the disk rim suggests that its activation mechanism involves a coupling between retinal RyR and the cGMP-gated channel.

Introduction

The cytosolic Ca^{2+} concentration ($[Ca^{2+}]_i$) regulates a wide range of cellular activities (Berridge *et al*., 2000; Carafoli *et al*., 2001). $[Ca^{2+}]_i$ itself is regulated through Ca^{2+} release channels and pumps located in the endoplasmic reticulum (ER) membranes (Berridge *et al*., 2000). Release of Ca^{2+} from the ER is mediated mainly by the inositol 1,4,5-trisphosphate ($InsP_3$) and ryanodine receptors (RyR; Banerjee & Hasan, 2005). RyRs exhibit intrinsic ryanodine-sensitive Ca^{2+} release channel activity and are modulated not only by Ca^{2+} but also by adenine nucleotides, caffeine, calmodulin and Mg^{2+} (Coronado *et al*., 1994; Meissner, 1994; Shoshan-Barmatz & Ashley, 1998; Treves *et al*., 2005). Three RyR types (types 1–3), sharing 65–70% overall identity in amino acid sequence, have been identified (Coronado *et al*., 1994; Meissner, 1994; Shoshan-Barmatz & Ashley, 1998). RyR1 and RyR2, originally described as skeletal- and cardiac muscle-specific types, were later detected in a variety of other tissues, with RyR2 being relatively abundant in brain and kidney. Four RyR subunits associate to comprise the functional RyR/Ca^{2+} release channel (Lai *et al*., 1989; Shoshan-Barmatz *et al*., 1995; Shoshan-Barmatz & Ashley, 1998).

In the vertebrate retina, dynamic changes in $[Ca^{2+}]_i$ control transduction and transmission of the visual signal at all stages of processing (Krizaj *et al*., 1999; Fain *et al*., 2001; Akopian & Witkovsky, 2002; Hurtado *et al*., 2002; Krizaj & Copenhagen, 2002; Chavez *et al*., 2006; Suryanarayanan & Slaughter, 2006). This is especially true in photoreceptor outer segments, where cytosolic $[Ca^{2+}]$ critically affects adaptation by modulating every step in the phototransduction cascade. In retina, calcium is regulated mainly by the activities of the cyclic nucleotide-gated (CNG) channel and the Na^+/Ca^{2+}–K^+ exchanger (Yau, 1994; Baehr & Palczewski, 2002). Accumulating research has shown that calcium concentration may also be regulated by uptake to and release from photoreceptor disks (Liebman, 1974; Kaupp *et al*., 1981; Schroder & Fain, 1984; Davis *et al*., 1988; Schnetkamp & Szerencsei, 1993; Panfoli *et al*., 1994; Schnetkamp, 1995; Wang *et al*., 1999). While much effort has been devoted to identifying the calcium uptake and release proteins in retina (see review by Krizaj & Copenhagen, 2002), RyR, a major calcium release channel, has been localized to retina mainly in lower vertebrates. In turtle, RyR was localized to the somas of most neurons, although the RyR isoform was not identified (Akopian *et al*., 1998). In salamander, RyR2 was mainly localized to photoreceptor inner segments and to the inner and outer plexiform layers (Krizaj *et al*., 2003; Krizaj *et al*., 2004). Studies addressing retinal RyR in mammals have, thus far, been restricted to bovine, where all three known types of RyR are expressed. However, as the ryanodine-binding properties are different from those of the known RyRs, retina probably expresses a novel isoform of RyR (Shoshan-Barmatz *et al*., 2005). The goal of this study was to further identify and localize RyR in mammalian retinas. We demonstrate that the major RyR isoform expressed in rabbit retina is a variant of RyR2, exhibiting two deletions and a single insertion. These changes may account for the distinct ryanodine-binding properties of retinal RyR. Retinal RyR is, moreover, localized to ER and photoreceptor disk rim, suggesting functional coupling with the cGMP-gated channel.

Correspondence: Dr Varda Shoshan-Barmatz, as above.
E-mail: vardasb@bgu.ac.il

Received 10 July 2006, revised 3 October 2007, accepted 5 October 2007

Materials and methods

Materials

3,3′-Diaminobenzidine (DAB), 2,4-dintrofluorobenzene (DNDFB), EDTA (ethylene-diaminetetraacetate), ethylene glycol bis (aminoethylether) tetraacetate (EGTA), Hepes, 3-(N-morpholino) propanesulphonic acid (MOPS) and Tris were obtained from Sigma (St Louis, MO, USA). [^{3}H]ryanodine (60 Ci/mmol) was purchased from NEN Life Science (Boston, MA, USA). Unlabelled ryanodine was obtained from Calbiochem (Darmstadt, Germany). A human *RyR2*-containing vector was a gift from Dr A. Marks (Columbia University). A monoclonal antibody (34C) recognizing all RyR types (Airey *et al*., 1990) was purchased from the Developmental Studies Hybridoma Bank (University of Iowa), polyclonal rabbit antibodies against the deduced C-terminal sequence (PAGDCFRKQYEDQLS) of skeletal muscle RyR (McPherson *et al*., 1991; conserved in RyR2 and RyR3) were purchased from Upstate Biotechnology (Lake Placid, NY, USA), and guinea pig polyclonal antibodies were prepared against purified rabbit skeletal muscle RyR (Zarka & Shoshan-Barmatz, 1993). Antibodies against RyR2 included a polyclonal, affinity-purified antibody preparation specific to canine cardiac RyR2 (kindly provided by Dr S. Fleischer, Vanderbilt University), and MA3-916, a monoclonal anticardiac RyR2 antibody from Affinity Bioreagents (ABR; Golden, CO, USA) that also recognizes RyR1 (Lai *et al*., 1992). Three polyclonal antibodies against RyR3 (all raised in rabbit) were tested. One antibody was developed against a purified glutathione-*S*-transferase fusion protein corresponding to the D1 region, showing low homology between the transmembrane domains 4 and 5 of RyR3 and other RyR isoforms (Giannini *et al*., 1995) and donated by Dr V. Sorrentino (University of Siena). The second antibody was a gift from Dr V. Sukumar (Health Sciences Center, University of Colorado, Denver) while the third came from Dr G. Meissner (University of North Carolina). An anticGMP-gated channel monoclonal antibody was a gift from Dr R. S. Molday (University of British Columbia). Horseradish peroxidase (HRP)-conjugated antimouse and antirabbit antibodies were from Protos Immunoresearch (San Francisco, CA, USA). fluorescein isothiocyanate (FITC)-labelled antirabbit antibodies were from Jackson Immunoresearch (West Grove, PA, USA). Secondary antibodies and protein A conjugated to alkaline phosphatase came from Promega (Madison, WI, USA).

Membrane preparations

Retinal membranal fractions were prepared from frozen bovine or rabbit retina (10 eyes) by homogenization in a motor-driven glass–Teflon homogenizer (10 strokes at 1000 r.p.m.) in a homogenization buffer containing 0.32 M sucrose, 10 mM Hepes, pH 7.4 and 0.1 mM PMSF (phenylmethylsulphonyl fluoride), with 0.5 μg/mL leupeptin and 0.5 μg/mL aprotinin as protease inhibitors. The homogenate was centrifuged at 1000 ***g*** for 15 min, and the obtained supernatant was centrifuged at 10 000 ***g***. The supernatant was further centrifuged for 30 min at 44 000 ***g*** and the pellet, termed P44, was resuspended in the homogenization buffer. The supernatant was centrifuged for 30 min at 160 000 ***g*** and the pellet, termed P160, was resuspended in the homogenization buffer. The P44 and P160 fractions contained no cytochrome c, a mitochondrial protein, but possesed ATP-dependent Ca^{2+}-uptake and ryanodine-binding activities, characteristic of ER membranes. In some experiments, bovine serum albumin (0.1%) was present until the final step when the membranes were resuspended in buffer without bovine serum albumin. The outer segment fraction was isolated as described previously (Panico *et al*., 1990). Sarcoplasmic reticulum membranes were prepared from rabbit fast-twitch skeletal muscle (Saito *et al*., 1984) and from rabbit cardiac tissue (Chamberlain *et al*., 1983), as described previously. Protein concentrations were determined by the standard Lowry procedure (Lowry *et al*., 1951). All membranes were frozen in liquid nitrogen and stored at −80 °C.

Gel electrophoresis and immunoblot analysis

Analysis of protein profiles by SDS–polyacrylamide slab gel electrophoresis (SDS-PAGE) was performed according to Laemmli (1970), using a gradient of 3–6% or 3–10% (w/v) acrylamide. Gels were stained with Coomassie blue or electrophoretically transferred onto nitrocellulose membranes (Towbin *et al*., 1979). The membranes were then incubated with a primary antibody followed by alkaline phosphatase- or HRP-conjugated antimouse, antiguinea pig antirabbit antibodies, or protein A, as appropriate. The blots were then processed for alkaline phosphatase detection or for enhanced chemiluminescence and exposed to X-ray film when HRP detection was required.

Oligonucleotide primers and reverse transcription (RT)-PCR amplification

Total RNA was prepared from rabbit retina using a DNA and RNA purification Kit (Epicentre, Madison, WI, USA). RT reactions were carried out at 30 °C for 10 min, followed by incubation at 45 °C for 45 min with 1–2 μg of total RNA in a 20 μL buffer containing 50 mM Tris-HCl, pH 8.3, 40 mM KCl, 5 mM $MgCl_2$, 0.5% (v/v) Tween 20, 1 mM DTT and 1 mM of each dCTP, dGTP, dTTP and dATP, 1 U/μL RNase inhibitor, 400 pmol random hexamer, and 50 U of Expand reverse transcriptase (Roche). PCR amplification of cDNA was performed using a series of specific primers designed for rabbit *RyR2* (Table 1). Amplification products were purified using a Gel Band purification kit (Amersham) followed by ligation into the pGEM-T easy vector (Promega, Madison, WI, USA) and then transferred into *E. coli XL-1* blue or DH5α cells. Bacterial colonies were analysed for plasmid uptake by PCR using primers specific for either the SP6- and T7-promoter regions or *RyR2*. Alternatively, colonies incorporating the PCR products were analysed on 1% (w/v) agarose gels, and colonies that contained an insert of the appropriate size were identified and sequenced. Some PCR fragments were also resolved on 15% (w/v) polyacrylamide gels and visualized by ethidium bromide staining.

Real-time PCR

Total RNA (1 μg) isolated from rabbit retina was reverse-transcribed using an Invitrogen kit. Primers for real-time quantitative PCR (Table 1) were designed using Primer Express software 2.0 (Applied Biosystems, Foster City, CA, USA) and synthesized by Sigma–Genosys. Real-time quantitative PCR was carried out using AB 7300 Sequence Detection Software (Applied Biosystems), using SYBR Green master mix reagent (Applied Biosystems) according to the manufacturer's instructions. The threshold cycle (Ct) was defined as the number of cycles required for the fluorescence intensity to rise above the background fluorescence. A standard curve was generated for each set of primers using different amounts of cDNA, and plotting Ct as a function of the amount of total cDNA added to the reaction. Mean Ct was obtained for each RyR isoform and ΔCt was calculated relative to RyR1 ($\Delta Ct = Ct_{isoformX} - Ct_{RyR1}$). Relative quantity was defined as $2^{\Delta Ct}$. To control for DNA contamination, total RNA was used.

TABLE 1. Primers used for retinal RyR2 RNA amplification

Primer	Location on cDNA	Sequence 5′-3′	Predicted PCR fragment length (bp)
RyR1-Fa	1098–1119	CTCATCCTTGTCAGCGTCTCCT	102
RyR1-Ra	1179–1199	CATGTTCCACAGGGTCTGCAT	
RyR2-Fa	1060–1081	GAAGAGCAACGGAGGACTGTTC	101
RyR2-Ra	1139–1160	CTTCCACTCCACGCAACTCTTA	
RyR2-Fb	11479–11499	TACCAGCAAGCCAGACTCCAT	102
RyR2-Rb	11560–11580	CAAAGTGGCAGCTACCATTGG	
RyR3-Fa	1431–1451	GGAGGAGATGCAGCATGAAGA	102
RyR3-Ra	1512–1532	CAATTCAACACCAAGGCCAAC	
RyR3-Fb	11136–11157	GCAGTCTTGCAGTGTCCTTGAT	103
RyR3-Rb	11217–11238	ACGCTCACGAACAATGAGTGTT	
F1	285–299	GAGGAGGCGCGGAGC	645
R1	914–930	CGTCTGCTGGAAGGCGG	
Fd	546–561	GGCTAACACGGTGGAG	87 (65)
Rd	619–633	CGATGGCCACCACC	
F2	930–944	GCTCTGGAGCGTGGC	1078
R2	1993–2008	CCGAGGAAGCTTCCAG	
F3	1903–1918	GAGTTGTTGGCGGCTC	1618
R3	3502–3521	CTGGCAGCATGATCTTGATC	
F4	3519–3534	CAGAGCCGAAGTGTGC	1930
R4	5433–5449	CAGTGGCGTAGGAGCTG	
F5	5450–5466	CCAGGCTCATGATGAAC	1076
R5	6509–6526	CAATGACAGACTCTTGGG	
F6a	6374–6393	TTAGAGGACGACTGCTTTCG	1100
R6a	7455–7474	AGGTCATGATTGCATTCCCC	
F6b	7412–7432	AAACACTTGATACGGAGGAGG	2096[a]
F7	8411–8427	CACAACCTGTTGATACC	1097
R7	9492–9508	CCAGATCCTCCGCAGCG	
F8a	9422–9441	TGGATGCAAGGACTGTGATG	927
R8a	10339–10357	CAGCCTCTGACATATCCCC	
F8b	10164–10183	CTTGGGAATTGATGAGGGAG	912
R8b	11057–11076	GAGTAACTTGTGCCATACGG	
F9	10941–10960	GACAGTGGAAAGAGTATTGG	1099
R9	12021–12040	CTACTTGTATAGCTTTGGAG	
Fi	11409–11423	GGAAGATGATGATGG	95 (119)
Ri	11489–11504	GGTCATGGAGTCTGG	
F10	12023–12040	CCAAAGCTATACAAGTAG	1330
R10	13339–13353	CTCCCCTTCCTCTCC	
F11a	13279–13299	AAAGTTGCAGAACTCTTAGCC	1059
R11a	14179–14197	CCCACTGGCCTTTAATATC	
F11b	14062–14082	TGCATCATTGGATACTACTGC	755
R11b	14800–14817	ATC TCC TGC TGG GTC TTC	
F12	14604–14621	GCTTGTATTAACTGTTGG	628
R12	15219–15232	CAGAGGTGCTGAGG	

Primers specific for *RyR2* used for Real-Time PCR (the first 10 primers, labelled with RyR) and for sequencing retinal *RyR*. Location of primers and size of the expected PCR product are given in the respective columns; the numbers in parentheses indicate the obtained fragment size when different from the expected. As positive control, all primers were also used to amplify human RyR2 (Otsu *et al*., 1990); 'a' indicates the predicted sequence length for a PCR fragment using primers F6b and R7.

Light-microscopic immunocytochemistry

Eyes from an adult rat, mouse or rabbit were removed under deep anaesthesia: for rat and rabbit, pentobarbital (45 μg/g); ketamine (40 mg/g) and xylazine (8 mg/g); and for mouse, a mixture of 85 μg/g ketamine and 13 μg/g xylazine. Drugs were injected intraperitoneally. Animals were killed by anaesthetic overdose (3× the initial dose). Animals were treated in compliance with federal regulations and University of Pennsylvania policy. Bovine eyes were obtained from local slaughterhouse either in Pennsylvania or Israel. Bovine, rat, mouse and rabbit eyecups were removed from anaesthetized adults and fixed in 4% (w/v) paraformaldehyde in phosphate buffer (PB; 0.1 M Pi, pH 7.4) for 1 h. In certain experiments, fixation strength or time was reduced to better retain antigenic sites. Following cryoprotection by incubation overnight in 30% sucrose in PB at 4 °C, retina was separated from the back of the eye, frozen in liquid nitrogen and sectioned radially (12 μm thickness) with a cryostat. For immunocytochemical staining, sections were incubated for 1 h in a blocking solution [PB containing 5% sucrose (SPB), 10% normal goat serum (NGS) and 0–0.4% Triton-X-100 for antibody 34C]. The sections were then incubated with the primary antibody (diluted in blocking solution) for 16–20 h at 4 °C. Following three washes with SPB, the sections were incubated for 2 h with secondary antibodies conjugated to FITC (for visualization by confocal microscopy) or to HRP and developed with DAB (0.5 mg/mL) and 0.015% hydrogen peroxide (for visualization by light microscopy). The sections were washed again and mounted with Vectashield (Vector Laboratories, Burlingame, CA, USA). Imaging was carried out by both conventional and confocal microscopy.

Electron-microscopic (EM) immunocytochemistry

Pre-embedding immunohistochemistry was carried out as described previously (Shoshan-Barmatz *et al*., 2004). Following fixation with 4% paraformaldehyde and cryoprotection, retina was embedded in agar and slices were sectioned at 70 μm with a Vibrotome. The

sections, now in 30% SPB, were repeatedly frozen (three or four times) in liquid nitrogen and thawed to facilitate the subsequent penetration of reagents. Floating sections were incubated in 10% NGS diluted in PB for 60 min at room temperature, and then with the primary antibody diluted in the blocking buffer overnight at 4 °C. After washing, sections were incubated for 2 h with HRP-conjugated Fab fragments. Sections were first incubated with DAB for 5–10 min, and then for up to 30 min with a fresh DAB solution containing 0.015% hydrogen peroxide. The DAB reaction product was amplified using the gold-substituted, silver-intensified peroxidase method (van den Pol, 1988). The sections were then postfixed in 2.5% (v/v) glutaraldehyde, osmicated in 2% (v/v) OsO_4, dehydrated, and embedded in Epon. Ultra thin sections (silver–gold) were mounted on formvar-coated slot grids, stained lightly with uranyl acetate and then examined in a JEOL 1010 electron microscope.

[^{3}H]Ryanodine binding

Retinal microsomal or sarcoplasmic reticulum (SR) membranes were incubated for 20 and 60 min at 30 °C and 37 °C, respectively, in a standard binding solution containing 1 M NaCl, 20 mM MOPS, pH 7.4, 50 μM free [Ca^{2+}] and 20–40 nM [^{3}H]ryanodine. Unbound ryanodine was separated from protein-bound ryanodine by vacuum filtration of the sample through nitrocellulose filters (0.3 μm) followed by two washes with 4 mL ice-cold buffer containing 0.2 M NaCl, 10 mM MOPS, pH 7.4, and 50 μM $CaCl_2$. The radioactivity retained on the dried filters was determined by liquid scintillation counting. Specific binding of [^{3}H]ryanodine is defined as the difference between the binding in the presence and absence of 100 μM unlabelled ryanodine.

Ca^{2+} accumulation

Retinal membranes and outer segments (0.2 mg/mL) were incubated in a reaction mixture containing 10 mM Mops, pH 6.8, 0.1 M NaCl, 3 mM $MgCl_2$, 3 mM ATP, 0.5 mM EGTA and 0.5 mM $CaCl_2$ (containing 3×10^4 cpm/nmol [$^{45}Ca^{2+}$]). After 5 min at 30 °C, Ca^{2+} uptake was terminated by rapid filtration (0.45 μm nitrocellulose filters) followed by a wash with 5 mL of 0.15 M NaCl. The radioactivity retained on the dried filters was determined by liquid scintillation counting.

Results

Retina expressed all three types of RyR

In earlier work, we showed that retina transcribes genes encoding all three types of RyR but that a monoclonal pan-RyR antibody which recognizes all three types cross-reacted with only one band, which had a mobility similar to that of RyR2 (Shoshan-Barmatz *et al*., 2005). We further showed that the retinal protein expressed distinct ryanodine-binding properties. Here, to better characterize the retinal RyR proteins, we analysed the interaction of six different anti-RyR antibodies with membranal fractions isolated from bovine or rabbit retinas and compared such interactions with those of skeletal and cardiac muscle SR.

In the retinal preparations (P44 and P160), the antibody raised in guinea pig against the rabbit RyR1 (Zarka & Shoshan-Barmatz, 1993) recognized a minor band with the same mobility as the skeletal muscle RyR1 monomer, confirming the expression of RyR1 in retina (Fig. 1A). Unexpectedly, this antibody also recognized a major band with mobility like that of RyR2 or RyR3. When retinal membranes were immunoblotted with two monoclonal antibodies that recognize all RyR types (34C and anti-C-terminus antibodies; Airey *et al*., 1990; McPherson *et al*., 1991), cross-reactivity with a single protein band in the position of RyR2 or RyR3 was observed (Fig. 1B and C). Similarly, a monoclonal antibody that recognizes RyR2 and, to a lesser extent, RyR1 (Lai *et al*., 1992) cross-reacted with a retinal protein with a mobility like that of RyR2 (Fig. 1D). These interaction patterns of the various antibodies thus suggest

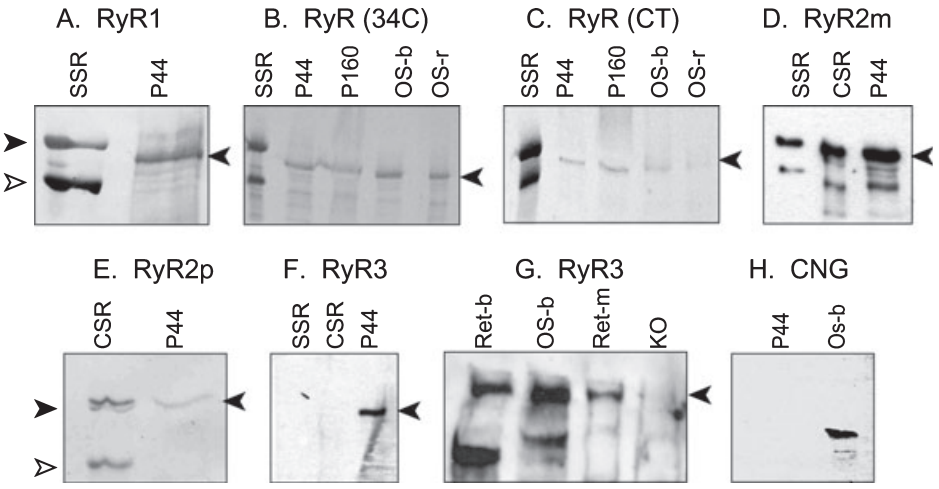

FIG. 1. Electrophoretic profile and immunoreactivity of RyRs in retinal membranal fractions, skeletal muscle SR and cardiac muscle SR. Bovine (Ret-b) and mouse (Ret-m) homogenates, bovine retinal fraction pellet 44 000 ***g*** (P44), pellet 160 000 ***g*** (P160), outer segment isolated from bovine (OS-b) or rabbit (OS-r) retina, skeletal muscle SR (SSR) and cardiac muscle SR (CSR) membranes were subjected to SDS-PAGE in 3–6% (w/v) acrylamide followed by immunoblot analyses. Western blotting was carried out as described under Materials and Methods using: (A) guinea-pig polyclonal anti-RyR1 antibodies (1 : 500); (B) monoclonal antibody 34C that recognizes all types of RyR (1 : 7500); (C) polyclonal antibody against a C-terminal peptide common to all isoforms (1 : 2000); (D) monoclonal antibody recognizing RyR2 (MA3-916) and to a lesser extent RyR1 (RyR2m); (E) purified polyclonal anticardiac muscle RyR2 (RyR2p); (F and G) anti-RyR3 (from Sorrentino 1 : 3000); and (H) an antibody against the photoreceptor CNG channel. To each lane the following protein amounts were applied (in μg): SSR (10), CSR (30), P44 (150), bovine or rabbit OS (50) except in G and H (10), and retinal homogenates (ret-b and ret-m in G; 10). Note that in retinal fractions in A–E, all antibodies revealed a band with an electrophoretic mobility of RyR2 or RyR3 and occasionally degradation products. Western blots were repeated 3–10 times with similar results. Closed arrowheads point to RyR and open arrowheads point to the RyR degradation product.

that RyR1 is not the major RyR isoform in retina. Indeed, an affinity-purified antibody specific against RyR2 cross-reacted with a retinal protein band with electrophoretic mobility like that of cardiac RyR2 (Fig. 1E). An antibody prepared against RyR3, which did not cross-react with either RyR1 or RyR2 in muscle SR, also labelled a protein band at the expected mobility for RyR3 (Fig. 1F). This anti-RyR3 antibody was also tested on retinas of wild-type and RyR3-knockout strain mice (Takeshima *et al*., 1996). A protein band of the expected mobility in the wild-type but not the knockout mouse confirmed that the observed band is indeed RyR3 (Fig. 1G).

Immunoblotting further revealed that RyR with the same electrophoretic mobility as RyR2 or RyR3 was also present in highly purified photoreceptor outer segments isolated from either bovine or rabbit retina (Fig. 1B and C). While we could not determine whether RyR1 or RyR2 is present in the outer segments, our experiments clearly showed that RyR3 is present (Fig. 1G). The purity of the outer segment preparation was confirmed using an antibody against the cGMP-gated channel (CNGC). While the CNGC was hardly detected in the P44 membranal fraction, it was readily detected in the outer segment preparation (Fig. 1H). Together, these experiments suggest that, while all three types are expressed by retina, the major retinal RyR corresponds to RyR2 or RyR3. However, as the retinal protein also unexpectedly interacted with antibodies raised against rabbit skeletal muscle RyR1 (Fig. 1B), it most probably represents a retina-specific RyR variant.

To test whether retinal RyR exists as a tetramer, as are all known RyR isoforms (Lai *et al*., 1989; Shoshan-Barmatz *et al*., 1995), chemical cross-linking of retinal membranes was carried out. Incubation of the retinal P44 membranal fraction with relatively low concentrations of the cross-linking reagent 1,5-difluoro 2,4-dinitrobenzene (DFDNB) and blotting with antibody 34C, raised against RyR, resulted in reduction of the RyR monomer protein band (closed arrow in Fig. 2) with a concomitant appearance of new bands of higher molecular masses (Fig. 2). These novel protein bands correspond to intramolecular cross-linked monomers ('a'), dimers ('b'), and tetramers ('c' in Fig. 2) of RyR subunits. As reported for other tissues, trimers were not observed (Shoshan-Barmatz *et al*., 1995). For comparison, similar cross-linking experiments were performed with SR membranes. The results thus indicate that retinal RyR is similar to all known RyR isoforms.

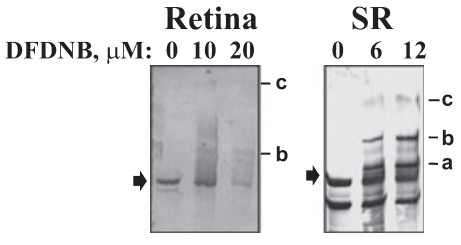

FIG. 2. Retinal RyR has a tetrameric structure. Retinal P44 membranal fraction or SR membranes (1 mg/mL) were incubated for 15 min at 37 °C with the indicated concentration of the cross-linking reagent 1,5-difluoro 2,4-dinitrobenzene (DFDNB) in 20 mM Tricine (N-(2-hydroxy-1, 1-bis (hydroxymethyl)-ethyl)-glycine), pH 8.0. Aliquots (40 μg) of the treated membranes were subjected to SDS-PAGE (3–8% acrylamide) followed by immunoblot staining using 34C anti-RyR antibody. Bands a–c indicate cross-linking products: intramolecular cross-linked monomers, dimers and tetramers, respectively.

The predominant RyR type in retina was a novel variant of RyR2

To identify the major RyR type expressed in retina, we carried out real-time PCR on cDNA prepared from total RNA isolated from rabbit retinas. Using two sets of primers specifically selected for each RyR isoform, and located in two different regions of the RyR sequences (Table 1), we found that RyR2 expression level was 10-fold higher than that of RyR1 and five-fold higher than that of RyR3 (Fig. 3). These differences were highly significant ($P < 0.05$, $n = 9$ for each isoform).

The unique ryanodine-binding properties of the retinal RyR (Table 2 and Shoshan-Barmatz *et al*., 2005), its unique peptide map (Shoshan-Barmatz *et al*., 2005) and its antibody reactivity profile suggest that retina expresses a distinct protein, albeit with a molecular mass (Fig. 1) and tetrameric structure (Fig. 2) similar to known RyR isoforms. However, as the major retinal RyR protein displays the same electrophoretic mobility as that of RyR2, and as real-time PCR showed that RyR2 is the major RyR isoform expressed in retina, we considered the possibility that the retinal RyR2 is a variant of the known RyR2.

To reveal the molecular identity of retinal RyR2, we designed sets of specific primers against various positions in rabbit *RyR2* cDNA (see Table 1). In this manner, the entire retinal RyR2 gene (~ 15 kbp) was sequenced (Fig. 4). The *RyR2* PCR product amplified with the F1-R1 primer pair lacked a 21-bp (seven amino acids) stretch located between base pairs 273 and 294 (Q92–W98) of RyR2 (Fig. 4). Open reading frame analysis of the F1-R1 600-bp fragment indicated that this deletion did not affect the original reading frame of the full-length gene. To gain insight into the relative abundance of this smaller gene fragment relative to the comparable fragment expected from RyR2, a second pair of primers (Fd, Road) was designed against this region. The obtained PCR product, separated on a polyacrylamide gel that can resolve small DNA sizes, was a major band of 66 bp (Fig. 4B, lane 1) and not the expected 87-bp band.

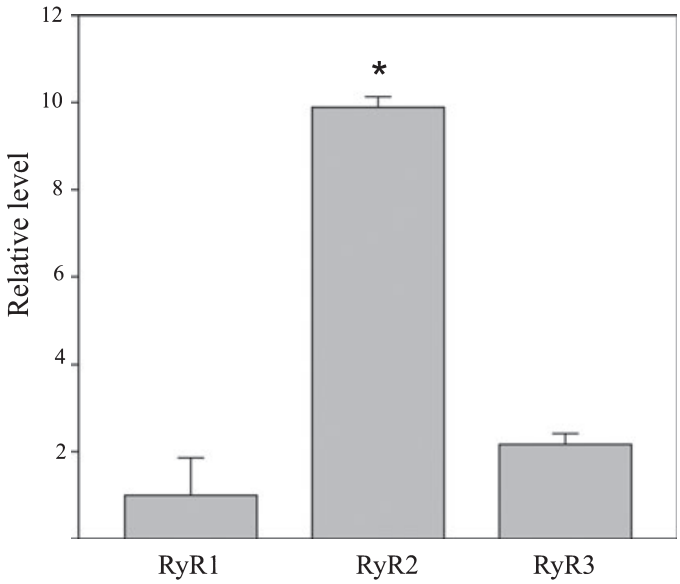

FIG. 3. RyR2 is the major type expressed in retina. Real-time PCR was performed as described in Materials and methods. Relative mRNA levels were measured using SYBR Green and calculated (using the Ct values) relative to RyR1. Data are the mean ± SEM and RyR2 was significantly more abundant than RyR1 or RyR3 (*$P \leq 0.05$). Two sets of primers for RyR types 2 and 3 and one set of primers for RyR1 were used (Table 1). Real-time PCR was carried out on three different retinal rabbit RNA preparations in triplicates for each set of primers.

Having cloned this region of the gene, we next employed additional primer pairs to map the rest of the gene. The PCR products obtained using a series of primer pairs (F2 to F8a forward and R2 to R8a reverse) yielded nucleotide sequences identical to those of rabbit *RyR2* between nucleotides 600 and 10954 (amino acids 200–3340). In the downstream sequence, however, a second modification in the retinal *RyR* gene was found. The PCR product generated using primer pair F9,R9 lacked a stretch encoding 12 amino acids (K3565–L3576) yet contained an insertion of eight amino acids encoded by the region between nucleotides 11149 and 11150 (corresponding to residues E3716–E3717), with the original reading frame of the full-length gene maintained. The insertion is probably present in all isolated preparations of rabbit retinal *RyR* mRNAs as it was found in all nine colonies tested. In addition, polyacrylamide gel electrophoresis of PCR products obtained using primers located at the edge of the identified insertion (Fi, Ri, Table 1) gave two PCR products of 95 and 119 bp, with the 119-bp product (corresponding to the insertion of 24 bp plus the expected 95 bp) being the major band (Fig. 4B, lanes 2 and 3). In summary, these studies indicate that retinal RyR shows > 99% identity to RyR2 in its translated nucleotide sequence but exhibits two deletions of seven and 12 amino acids and a single insertion of eight amino acids not found in RyR2 (Fig. 4C).

In retina, RyR2 was localized to the soma and primary dendrites of horizontal, amacrine and ganglion cells

Next, we wished to localize different types of RyR in retinal neurons, starting with the most abundant type. Immunostaining with the

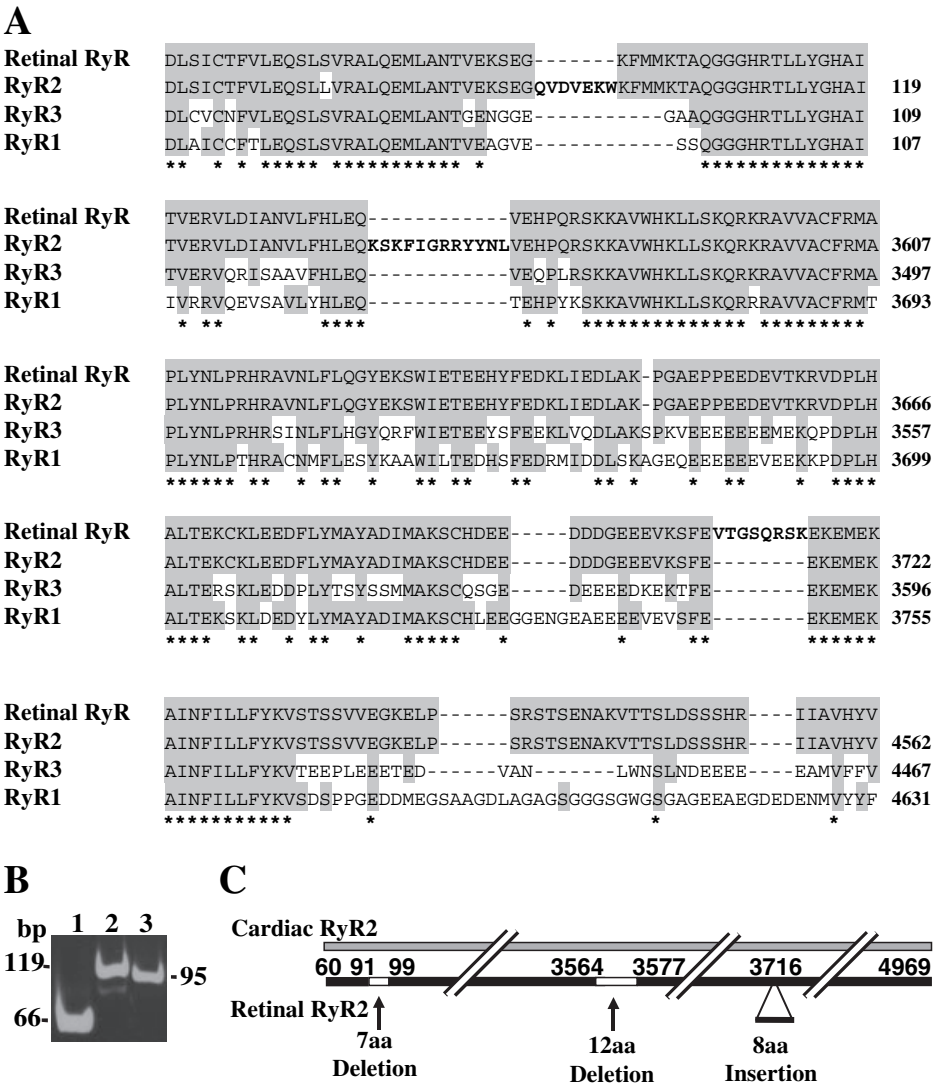

FIG. 4. Retinal transcript for RyR2 contains several modifications as compared to cardiac RyR2. (A) Multiple sequence alignment of retinal RyR2 amino acid sequences with rabbit cardiac RyR2 (Otsu *et al*., 1990), rabbit skeletal muscle RyR1 (Takeshima *et al*., 1989) and rabbit RyR3 (Hakamata *et al*., 1992). Selected sections of the sequence are compared and the amino acid residue numbers are indicated. The deletion and insertion presented were obtained in all colonies sequenced. RT-PCR analysis of specific RyR transcripts in retina was carried out as described under Materials and Methods and using the primers listed in Table 1. Gray boxes indicate amino acid sequences in retinal RyR identical to one of the RyR isoforms and the asterisk (*) indicates that the amino acid sequences were identical in all RyR isoforms. (B) PCR fragments were resolved on 15% (w/v) polyacrylamide gel and visualized by ethidium bromide staining. The bands represent PCR products amplified with the following primers: lane 1, Fd-Road (546–633 in nucleotide sequence), lane 2, Fi-Ri (11409–11507) and lane 3, Fi-Ri amplifing the pcDNA–human *RyR2* plasmid. (C) A schematic diagram representing the specific RyR2 transcript in retina. Gray and black boxes represent full-length rabbit *RyR2* and retinal RyR proteins, respectively. In the retinal RyR protein, deletions are indicated by open boxes while insertions are indicated by black boxes. Diagonal lines interupt identical sequences between the two variants.

affinity-purified anti-RyR2 antibodies gave staining in the outer plexiform, the inner nuclear and the ganglion cell layers, with staining being particularly strong in the soma of the horizontal, amacrine and ganglion cells (Fig. 5A). Horizontal cells showed staining for RyR2 in both the cell body and processes (Fig. 5B and E). In ganglion cells, staining was also present in the primary dendrites (Fig. 5B and C). Within the somas of these cells, staining appeared punctuate, suggestive of ER staining (Fig. 5D). The monoclonal anti-RyR2 antibodies did not reveal any staining and thus could not be used for immunolocalization.

To localize RyR3, we immunostained retina with three different antibodies; all gave different staining patterns which remained the same in the RyR3-null retina, indicating that the staining was nonspecific. Thus, it is currently impossible to localize RyR3 to retinal structures by immunostaining. We further tried to localize all RyRs by using several pan-antibodies. The C-terminus anti-RyR antibody revealed no staining. The widely used 34C anti-RyR antibody, when used on frog retina, gave strong staining in photoreceptor inner segments and in the inner plexiform layer, consistent with the reported staining in salamander (Krizaj *et al*., 2003, 2004). However, a variety of fixation and staining protocols applied to mammalian retinas (rat, bovine, guinea pig, mouse, monkey) revealed only a weak staining in the outer plexiform layer, presumably in horizontal cells' somas and processes (Supplementary material, Fig. S1). This suggests that antibody 34C does not recognize well the folded or fixed forms of mammalian RyRs.

Light, confocal, and electron microscopy revealed localization of RyR to photoreceptor outer segment disk rims

A polyclonal anti-RyR1 antibody applied to rabbit retinas (the same species against which the antibody was prepared) revealed strong staining in photoreceptor outer segments (Fig. 6A). Staining was also observed in somas of ganglion, amacrine and horizontal cells, and in the myoid region of the inner segment, a region packed with rough ER. The ellipsoid region, where mitochondria reside, was unstained. To test whether the obtained staining pattern held true for other mammals we also stained rat retina and found that the same cell types, i.e. ganglion, amacrine, horizontal and photoreceptors cells were stained in this species as well; the inner segments, however, appeared unstained (Fig. 6B). Pre-absorbing the antibodies with purified rabbit skeletal muscle RyR1 diminished the staining, suggesting that the labelling was specific for RyR (Fig. 6C and D).

The immunolocalization of RyR in the photoreceptor outer segments, as visualized by confocal microscopy, appeared as two parallel lines, one on either side of the outer segment, suggesting that the staining was restricted to the outer segment edge (Fig. 6A and E). Electron microscopy confirmed this observation and further revealed association of gold particles with the disk rim and possibly also with the plasma membrane (Fig. 7A and B). In ganglion cells, staining with this antibody was restricted to ER membranes, confirming the specificity of this antibody to RyR (Fig. 7C).

The ryanodine-binding properties of photoreceptor outer segment membranes were similar to those of retinal membranes

We have previously shown that the ryanodine-binding properties of retinal RyR differ from those of known RyR isoforms (Shoshan-Barmatz *et al*., 2005). The retinal fractions used in that earlier study contained membranes from all retinal neurons. Having now localized RyR to both inner retina and photoreceptor outer segments, we asked whether the RyR of the photoreceptor outer segments also possesses the same novel binding properties. We have thus isolated photoreceptor outer segments and compared their ryanodine-binding properties to membrane fractions isolated from whole retina or from skeletal and cardiac muscle (SR; Table 2). In contrast to skeletal and cardiac RyR, which show Ca^{2+}-dependent binding (Lai *et al*., 1992; Meissner, 1994; Shoshan-Barmatz & Ashley, 1998; Treves *et al*., 2005) similar to whole retinal membranes, binding of ryanodine to photoreceptor outer segments was independent of Ca^{2+}. As the high salt concentrations used in the ryanodine-binding assay contain free Ca^{2+} at a concentration sufficient to stimulate a high level of binding, Ca^{2+} requirement is demonstrated using EGTA to chelate the contaminating Ca^{2+}. While EGTA completely prevented ryanodine binding to skeletal and cardiac muscle SR it decreased binding to outer segment RyR only by 14–30%. In addition, again similar to that observed with whole retina, caffeine, known to stimulate ryanodine binding, inhibited rather than stimulated binding of [^{3}H]ryanodine to photoreceptors, and, while ruthenium red effectively inhibited binding to the SR (by ~ 80%; Lai *et al*., 1992; Meissner, 1994; Shoshan-Barmatz & Ashley, 1998), it blocked binding to the outer segments much less efficiently (by only ~ 20%).

TABLE 2. Ryanodine-binding properties of the outer segment are similar to those of retinal membranes but different from those of skeletal or cardiac muscle membranes

	Ryanodine bound, % of control			
Additions	SSR	CSR	P44	OS
EGTA (1 mM)	1.3 ± 4	3 ± 1	71 ± 8	86 ± 5
Caffeine (10 mM)	143 ± 10	ND	15 ± 3	13 ± 6
Ruthenium red (20 μM)	22 ± 4	64 ± 6	76 ± 6	81 ± 9

Retinal membranes (P44), 1.5 mg/mL, and outer segment disks (OS; 0.5 mg/mL) isolated from bovine retina, skeletal muscle SR (SSR), or cardiac muscle SR (CSR), 1 mg/mL, membranes were incubated in a reaction mixture containing 20 nM ryanodine, 0.5 M NaCl and 50 μM $CaCl_2$, and the indicated compound to test ryanodine binding. After 1 h at 37 °C, samples were assayed for bound [^{3}H]ryanodine, as described in Materials and Methods. Control activities with no added compound (100%) were (in pmol/mg protein): SSR, 3.9 ± 0.8 ($n = 4$); CSR, 1.03 ± 0.03 ($n = 3$); P44, 0.211 ± 0.21 ($n = 4$); and OS, 0.401 ± 26 ($n = 3$). Values are the mean ± SEM of $n = 3$ or 4 experiments.

ATP-dependent Ca^{2+} uptake by the P44 and outer segment fractions

The release of Ca^{2+} from its intracellular stores requires the prior accumulation of the ion in these stores by active Ca^{2+} transport, catalysed by Ca^{2+} pumps. Therefore, Ca^{2+} accumulation by the P44 retinal subcellular membranal preparations and the outer segment was tested (Table 3). As expected for vesicular Ca^{2+} accumulation, oxalate and Pi increased Ca^{2+} accumulation by the retinal membranes while the Ca^{2+} ionophore, A23187, decreased net Ca^{2+} accumulation (Table 3). We observed Ca^{2+}-dependent phosphorylation of a 100-kDa protein, corresponding to the phosphorylated intermediate form of the Ca^{2+} ATPase (data not shown), suggesting the presence of a P-type Ca^{2+} pump in the retinal membranal preparations. Although we did not identify the exact SERCA isoform present in bovine retina, the presence of a P-type Ca^{2+}-pump that mediates Ca^{2+} accumulation is in agreement with previous results (Davis *et al*., 1988; Panfoli *et al*.,

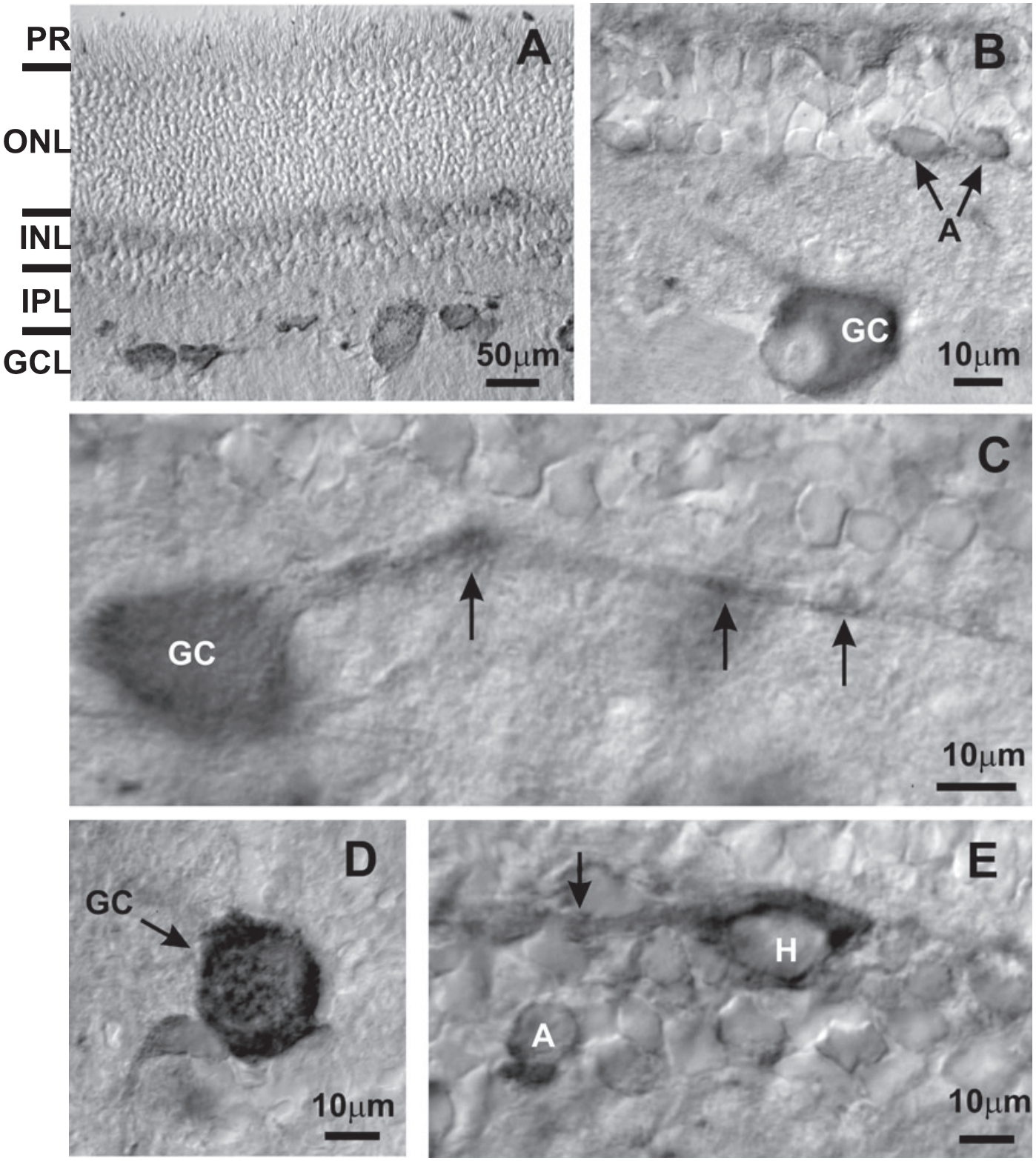

FIG. 5. Cardiac-type RyR was expressed by most cell types in bovine retina. Immunostaining of a cross-section of bovine retina with purified anti-RyR2 (cardiac) antibody (provided by S. Fliescher) was carried out as described in Materials and Methods and visualized with DAB reaction product. (A) Low magnification showing stain in the outer plexiform layer (between ONL and INL), inner nuclear layer (INL) and ganglion cell layer (GCL). (B–E) Higher magnification. Stain is present in somas of horizontal (H), amacrine (A) and ganglion (GC) cells, in ganglion cell dendrites (arrows in C) and in a horizontal cell processes (arrow in E). Note that staining in the ganglion cell's soma is punctate (D). For this and Fig. 6, PR, photoreceptor layer; ONL, outer nuclear layer; INL, inner nuclear layer; IPL, inner plexiform layer; GCL, ganglion cell layer.

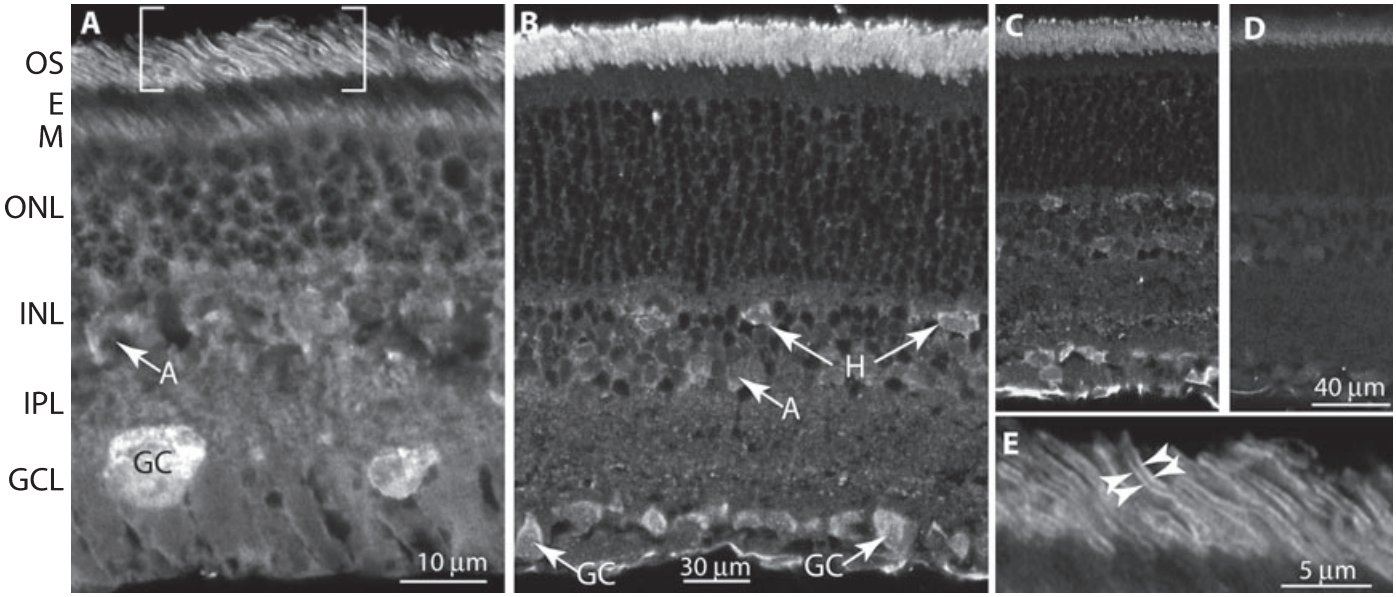

FIG. 6. RyR was localized to photoreceptor outer segments. Immunostaining using the guinea pig antiskeletal RyR and a secondary antibody conjugated to FITC; sections were imaged with a confocal microscope. (A) Rabbit retina; staining is present in outer segments (OS), myoid region of the outer segment (M), amacrine (A) and ganglion (GC) cell somas. (B) Rat; as in rabbit, immunostaining is strongest in outer segments, and is also present in horizontal (H), amacrine (A), and ganglion cells (GC). (C and D) Immunostaining of rat retina (C) was eliminated after preincubating the antibody with purified skeletal muscle RyR (D); these stainings were done in parallel. (E) The bracketed region in B was enlarged to show how the stain outlines the outer segments (arrowheads). Scale bar in D applies to C.

1994) and consistent with localization of SERCA3 to the cone outer segment (Krizaj, 2005), suggesting the presence of a Ca^{2+} pump in retinal ER and photoreceptor outer segment membranes.

Discussion

Retina expressed an alternative form of RyR2

Several pieces of evidence show that the major RyR expressed in retina is RyR2, though it is an isoform that differs from the known cardiac RyR2. In a previous study, we demonstrated that the tryptic map of RyR in ER-enriched retinal membranes was different from that obtained with both skeletal muscle RyR1 and cardiac RyR2 preparations (Shoshan-Barmatz *et al*., 2005). Moreover, the ER-enriched retinal membranal fraction displayed unique ryanodine-binding properties (Shoshan-Barmatz *et al*., 2005). Here, we examined the entire 15-kb coding region of retinal *RyR2* using rabbit retinal cDNA as template and found its sequence to be different from cardiac RyR2. Aligning RyR1, RyR2, RyR3 and retinal RyR2 sequences clearly showed that the amplified sequence is distinct from RyR1 and RyR3 yet >99% identical in its translated nucleotide sequence to RyR2 (Fig. 4). The modification in the retinal *RyR2* sequence, henceforth referred to as Ret-RyR2, includes a deletion of 21 bp, representing a slicing of exon 4 encoding a seven amino acid fragment (Q92–W98), a second deletion encoding 12 amino acids (K3565–L3576) and an insertion of eight amino acids (VTGSQRSK) found between residues E3716 and E3717 (Fig. 4). Similar 24-bp sequence insertions encoding the same amino acid sequence have been found in human, rabbit and dog cardiac RyR2 (George *et al*., 2007).

The new variant of RyR2 found here is the major RyR in retina because: (i) the major protein band labelled by anti-RyR antibodies recognizing all RyR isoforms migrated as RyR2 or RyR3 (Fig. 1); (ii) the major transcript in retina is RyR2 (Fig. 3); and (iii) almost all rabbit RyR2 transcripts analysed showed the same insertion and deletions identified as Ret-RyR2. The finding that Ret-RyR2 is the major RyR in mammalian retina is consistent with studies in salamander retina, where it was proposed that RyR2 is the major isoform based on immunostaining (Krizaj *et al*., 2003; Krizaj *et al*., 2004).

The unique retinal RyR ryanodine-binding properties may be explained by the modified Ret-RyR2 protein sequence

The unique ryanodine-binding properties found in retina include Ca^{2+}-independence (Table 2; Shoshan-Barmatz *et al*., 2005), fast association and dissociation of ryanodine, and inhibition, rather than stimulation, by caffeine (Shoshan-Barmatz *et al*., 2005). It is therefore reasonable to assume that sequence modification in Ret-RyR2 account for some of the unique ryanodine-binding properties of retinal RyR. It has been proposed that Ca^{2+} binding mediates conformational changes leading to exposure of the ryanodine-binding site of the protein (Coronado *et al*., 1994). It is possible therefore that in Ret-RyR2 the ryanodine-binding site is naturally exposed, leading to fast ryanodine association and dissociation and Ca^{2+}-independent ryanodine binding. The ryanodine- and Ca^{2+}-binding sites of RyR1 and RyR2 have not been localized. However, a single mutation in several locations in either RyR1 or RyR2 sequences was found to alter caffeine, Ca^{2+}- and ryanodine-binding affinity (Fessenden *et al*., 2004). Natural mutations that significantly alter RyR function and cause diseases tend to occur in three regions of RyR1 and RyR2. In RyR2, the first region is between amino acids 77 and 433 (Brini, 2004), which contains the first deletion we found here (Δ92–98). Therefore, it is possible that the identified modifications in the Ret-RyR2 sequence are responsible for the observed altered ryanodine-binding properties. Indeed, recent functional characterization of a human RyR2 splice variant that contains the same 24-bp insertion as Ret-RyR2 showed profound effects on organelle structure, Ca^{2+} signalling and susceptibility to

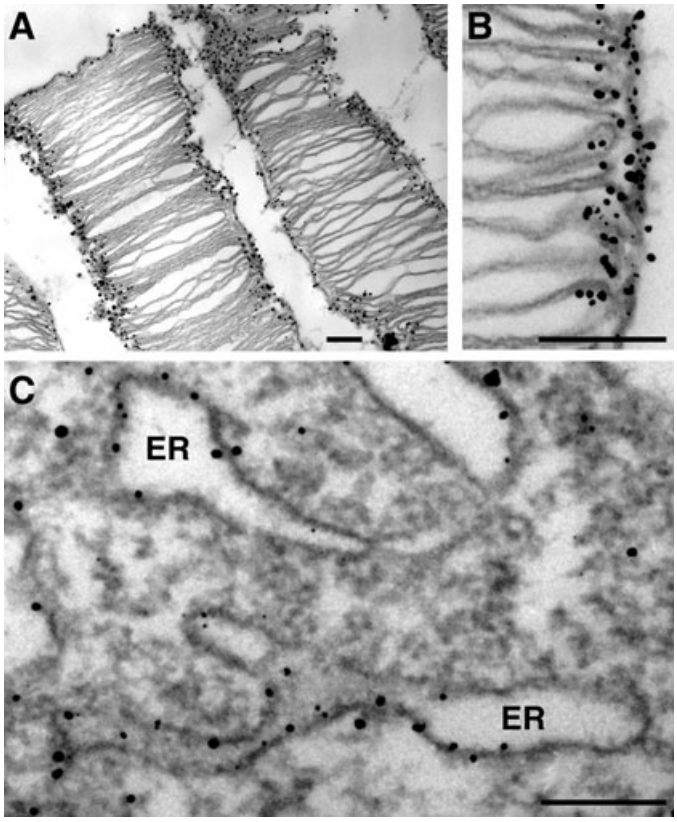

FIG. 7. RyR was localized to the ER in ganglion cell somas and to the rim of the photoreceptor disk membrane. Electron micrographs of rat retina immunostained with guinea pig anti-RyR1 and processed for electron microscopy using the silver-substituted gold intensification procedure. (A) Staining outlines rod outer segments. (B) At higher magnification of a different rod, stain is present on both the plasma membrane and rim region of the disk membrane. (C) In the cytosol of ganglion cell somas, stain is localized to the endoplasmic reticulum membranes. Note that most gold particles lie on the membrane. Scale bars, 200 nm.

TABLE 3. Ca^{2+} accumulation by P44 membranal fractions and outer segments

	Ca^{2+} accumulation, nmol/mg protein	
Additions	P44	OS
None	9.4 ± 1.7	10 ± 2
Pi (20 mM)	16.7 ± 2	17.7 ± 3
Pi (50 mM)	19.9 ± 3	23.7 ± 5
Pi (50 mM) + A23187 (5 μM)	3.0 ± 0.4	3.9 ± 2
Oxalate (2 mM)	13.5 ± 2.4	13 ± 2
Oxalate (5 mM)	14.5 ± 2	16 ± 3

Retinal membranes (P44) and outer segments (OS; 0.2 mg/mL) were isolated and assayed for Ca^{2+} uptake as described in Materials and Methods. The membranes were incubated for 5 min at 30 °C in a buffer containing ATP, $MgCl_2$ and Ca^{2+} (containing $^{45}Ca^{2+}$), as detailed in Materials and Methods. The indicated compound and the vesicles were separated from free Ca^{2+} by rapid filtration through 0.45-μm nitrocellulose filters and radioactivity trapped in the filter was counted. Numbers are mean ± SEM of three different experiments.

apoptosis (George *et al*., 2007). In particular, expression of this RyR2 spliced variant in HL-1 cardiomyocytes suppressed intracellular Ca^{2+} fluxes and protected cells from caffeine-induced apoptosis. Although the rabbit retinal RyR2 characterized in this study contains other modifications (two deletions), the strong link found between reduced RyR2-dependent Ca^{2+} fluxes in the 24-bp insertion human RyR2 splice variant and the protection from caffeine-induced apoptosis is consistent with our findings of Ca^{2+}-independent ryanodine binding and with the finding of ryanodine-binding inhibition rather than stimulation by caffeine. The precise mechanism for the differential Ca^{2+} release mediated by the distinct RyR2 splice variant is as yet unknown.

An important question aks if the majority of retinal RyR is Ret-RyR2 and, if Ret-RyR2 accounts for the unique ryanodine-binding properties observed in retinal preparation, how is it that most physiological experiments found stimulation of Ca^{2+} release by caffeine (Krizaj *et al*., 1999; Fain *et al*., 2001; Akopian & Witkovsky, 2002; Hurtado *et al*., 2002; Krizaj & Copenhagen, 2002; Chavez *et al*., 2006; Suryanarayanan & Slaughter, 2006)? One possible explanation is that RyR in synaptic regions is a known isoform with conventional ryanodine-binding properties but which does not contribute a large quantity of receptor to membrane preparations. Another possible explanation is that the ryanodine-binding assay of the novel retinal RyR does not reflect Ca^{2+} release *in vivo*.

Localization of RyR in retinal neurons

We have shown here that two antibodies, one raised against RyR1 and one against RyR2, labelled somas and primary dendrites of most retinal neurons, with little staining in the synaptic layers. Electron microscopy showed that, as expected for RyR, this labelling was associated with ER membranes, providing further evidence that the staining was specific. Similar localization of RyR to somas of most retinal neurons has also been described in turtle retina (Akopian *et al*., 1998). These staining patterns differ from that of salamander retina, which localized RyR2 to photoreceptor inner segments and both synaptic layers (Krizaj *et al*., 2003, 2004). Indeed, one would expect expression of RyRs in the synaptic layers as this receptor modulates a variety of synaptic activities such as $GABA_A$ response in ganglion cells (Akopian *et al*., 1998; Akopian & Witkovsky, 2002), certain glutamate responses in amacrine cells (Sosa *et al*., 2002) and transmitter release in many cell types including photoreceptor terminals and amacrine cells (Koulen *et al*., 1999; Hurtado *et al*., 2002; Krizaj *et al*., 2003; Chavez *et al*., 2006; Suryanarayanan & Slaughter, 2006). Clearly, localization of RyR in mammalian retina, as well as salamander in which a pan-antibody did not reveal staining in most retinal somas (Krizaj *et al*., 2004), is still incomplete.

RyR localization and possible function in the photoreceptor outer segments

Our results strongly suggest that photoreceptor outer segments express RyR. First, using an enriched outer segment preparation, two antibodies that recognize all types of RyR cross-reacted with a protein band that migrates on SDS gels as RyR2 or RyR3. Second, an antibody raised against RyR3 labelled the expected protein band in outer segment preparation. Third, isolated outer segment preparations from bovine and rabbit bound ryanodine, a property considered specific for RyR. Fourth, immunostaining with an antibody specific to RyR was associated with the outer segment disk membranes (Fig. 7). Expression of RyR is in agreement with a recent paper showing RyR bands in a preparation of isolated disk membranes (Panfoli *et al*., 2007).

Resolving which type of RyR is expressed by the outer segment is not so simple. The fact that the outer segment stains with our anti-RyR1 antibodies suggests that the outer segment expresses RyR1, and the fact that anti-RyR3 antibodies detect a band in the outer

segment preparation suggests that the outer segment expresses RyR3. However, as the outer segment ryanodine-binding properties differ from known RyR1 or RyR3, these would have to be variants of the known types. Furthermore, as these binding properties are similar to those of whole retina preparation, where the most abundant isoform is Ret-RyR2, it is possible that the outer segment actually expresses Ret-RyR2. Any combination of these receptors is also possible.

Regardless of RyR type, high resolution confocal and electron microscopy localized outer segment RyR to the rim of outer segments disks, and probably also to the plasma membrane. This distribution differs from that of the InsP3 receptor, which was localized along the whole length of the disk membranes (Wang *et al*., 1999). Other proteins, such as Peripherim/*rds* and Rom1, also specifically localize to the rim region of the outer segment disks, where they form complexes amongst themselves and with the CNG channel and the Na/Ca–K exchanger (Molday, 1998; Goldberg & Molday, 2000; Poetsch *et al*., 2001), the latter being essential for disk morphogenesis. It is possible that, in the outer segment, RyR associates with this complex to contribute and modulate its function.

Another possible function for RyR in the outer segment involves light adaptation. Regulation of phototransduction crucially depends upon $[Ca^{2+}]_i$, which modulates the activity of guanylyl cyclase-activating protein, calmodulin, protein kinase C and recoverin (for review see Hurley & Chen, 2001). It is generally thought that $[Ca^{2+}]_i$ is modulated mainly by CNG channels and the Na^+/Ca^{2+}–K^+ exchanger (Fain *et al*., 2001). However, several pieces of evidence suggest that the disks also contribute to Ca^{2+} homoeostasis in the outer segments. First, the outer segment shows ATP-dependent Ca^{2+}-uptake activity (Table 3; Panfoli *et al*., 1994; Krizaj *et al*., 2003; reviewed by Schnetkamp, 1995). Second, in the absence of extracellular Ca^{2+}, bright light increases intracellular calcium (Matthews & Fain, 2001; Cilluffo *et al*., 2004) and third, InsP3 can release Ca^{2+} from internal stores (Parker & Miledi, 1986; Schnetkamp & Szerencsei, 1993; Schnetkamp, 1995), consistent with immunoreactivity for $InsP_3$ receptors on cone outer segment disk membranes (Wang *et al*., 1999).

We suggest that RyR at the photoreceptor disk rim may contribute to local regulation of Ca^{2+} close to the plasma membrane, where the Na^+- and Ca^{2+}-permeable CNG channels reside (Fig. 8). If RyR operates via Ca^{2+}-induced Ca^{2+} release then a possible activation mechanism could involve Ca^{2+} permeating the cell through the CNG channel (as voltage-dependent Ca^{2+} channels are not present in the photoreceptor outer segments). This mechanism is similar to the proposed control mechanism of RyR2 (Coronado *et al*., 1994; Meissner, 1994; Shoshan-Barmatz & Ashley, 1998; Treves *et al*., 2005). However, because ryanodine binding, as a proposed reflector of the RyR channel's conformational state (i.e. open or closed; Coronado *et al*., 1994), is Ca^{2+}-independent, coupling between voltage changes in the plasma membrane and activation of Ca^{2+} release from the disk calls for a novel mode of activation.

It is tempting to speculate that functional coupling between the CNG channel and the RyR involves protein–protein interactions similar to the interaction between skeletal muscle RyR1 in the SR and the dihydropyridine receptor L-type Ca^{2+} channel in the transverse tubule, involved in excitation–contraction coupling (Franzini-Armstrong & Jorgensen, 1994; Liu *et al*., 1996). The functional linkage between the two proteins requires specific positioning of four dihydropyridine receptors (forming a tetrad), in correspondence with the four identical subunits of a single RyR1 channel. A similar control mechanism in which Ret-RyR is activated by the CNG channel is plausible because outer-segment RyR and the CNG channel are localized in close proximity in two adjacent membranes, and the sequence modifications found in Ret-RyR2 are shared with RyR1 and RyR3. In addition, as required for such functional coupling, both CNG channel and retinal RyR (Fig. 2) are tetramers (Kaupp & Seifert, 2002; Zheng *et al*., 2002). Thus, the model suggests that the CNG channel possesses cytoplasmic domains that

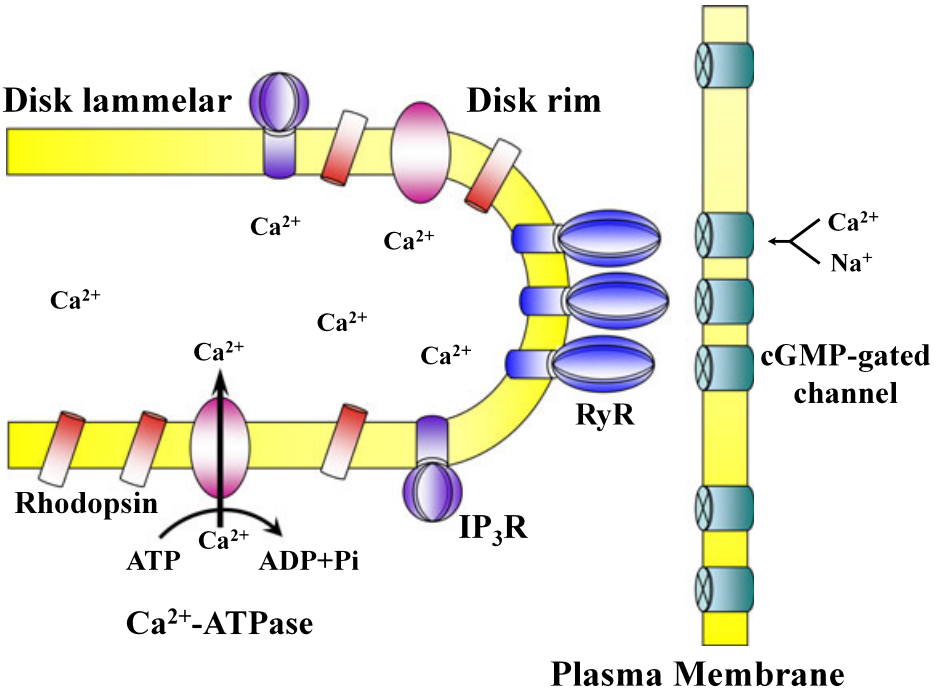

FIG. 8. A model illustrating the distribution of RyR, of cGMP-gated channels and of various proteins in the outer segment.The model shows the transmembrane topology of RyR at the disk rim and of the cGMP-gated channel in the plasma membrane. Both RyR and the CNG channel are tetramers. The Ca^{2+}-ATPase in the disk lamellar region is also shown. A possible modulation of the outer segment RyR by cGMP-gated channels is suggested.

could potentially interact with closely apposed outer segment RyR in the disk rim and modulate its activity (Fig. 8). The model does not suggest that all CNG channels are coupled in this fashion, only a percentage. Such coupling could contribute to calcium regulation at a slower rate than regulation by the CNG channel and the Na^+/Ca^{2+}–K^+ exchanger, and might be responsible for regulation during extreme lighting conditions.

Supplementary material

The following supplementary material may be found on http://www.blackwell-synergy.com

Fig. S1. The pan-RyR antibody 34C is not suitable for immunocytochemistry in mammalian retinas.

Acknowledgements

We thank Marie Fina for excellent technical assistance and Kevin Foskett (University of Pennsylvania) for reading the mansucript. We also thank the following people for antibody donations: Sidney Fleischer (Vanderbilt University; polyclonal anti-RyR2), Vincenzo Sorrentino (University of Siena; anti-RyR3), Vijayaraghavan Sukumar (University of Colorado at Denver and Health Sciences Center; anti-RyR3), Gerhard Meissner (University of North Carolina; anti-RyR3) and Robert S. Molday (University of British Columbia; anticGMP-gated channel). We thank Jianjie Ma (UMDNJ-Robert Wood Johnson Medical School) for contributing RyR3-knockout mice. This research was supported in part by a grant from the Israel-USA Binational Science Foundation (to V.S.B.) and by a NIH grant EY1105 (to N.V.).

Abbreviations

$[Ca^{2+}]_i$, cytosolic Ca^{2+} concentration; CNG channel, cyclic nucleotide-gated channel; Ct, threshold cycle; DAB, 3,3′-diaminobenzidine; EGTA, ethylene glycol bis (aminoethylether) tetraacetate; ER, endoplasmic reticulum; FITC, fluorescein isothiocyanate; HRP, horseradish peroxidase; $InsP_3$, inositol 1,4,5-trisphosphate; MOPS, 3-(N-morpholino) propanesulphonic acid; Pi, inorganic phosphate; RT-PCR, reverse-transcription PCR; RyR, ryanodine receptor; SDS-PAGE, sodium dodecyl sulphate–polyacrylamide gel electrophoresis; SR, sarcoplasmic reticulum.

References

Airey, J.A., Beck, C.F., Murakami, K., Tanksley, S.J., Deerinck, T.J., Ellisman, M.H. & Sutko, J.L. (1990) Identification and localization of two triad junctional foot protein isoforms in mature avian fast twitch skeletal muscle. *J. Biol. Chem.*, **265**, 14187–14194.

Akopian, A., Gabriel, R. & Witkovsky, P. (1998) Calcium released from intracellular stores inhibits $GABA_A$-mediated currents in ganglion cells of the turtle retina. *J. Neurophysiol.*, **80**, 1105–1115.

Akopian, A. & Witkovsky, P. (2002) Calcium and retinal function. *Mol. Neurobiol.*, **25**, 113–132.

Baehr, W. & Palczewski, K. (2002) *Photoreceptors and Calcium*. Springer, New York.

Banerjee, S. & Hasan, G. (2005) The InsP3 receptor: its role in neuronal physiology and neurodegeneration. *Bioessays*, **27**, 1035–1047.

Berridge, M.J., Lipp, P. & Bootman, M.D. (2000) The versatility and universality of calcium signalling. *Nat. Rev. Mol. Cell Biol.*, **1**, 11–21.

Brini, M. (2004) Ryanodine receptor defects in muscle genetic diseases. *Biochem. Biophys. Res. Commun*, **322**, 1245–1255.

Carafoli, E., Santella, L., Branca, D. & Brini, M. (2001) Generation, control, and processing of cellular calcium signals. *Crit. Rev. Biochem. Mol. Biol.*, **36**, 107–260.

Chamberlain, B.K., Levitsky, D.O. & Fleischer, S. (1983) Isolation and characterization of canine cardiac sarcoplasmic reticulum with improved Ca^{2+} transport properties. *J. Biol. Chem.*, **258**, 6602–6609.

Chavez, A.E., Singer, J.H. & Diamond, J.S. (2006) Fast neurotransmitter release triggered by Ca influx through AMPA-type glutamate receptors. *Nature*, **443**, 705–708.

Cilluffo, M.C., Matthews, H.R., Brockerhoff, S.E. & Fain, G.L. (2004) Light-induced Ca^{2+} release in the visible cones of the zebrafish. *Vis. Neurosci.*, **21**, 599–609.

Coronado, R., Morrissette, J., Sukhareva, M. & Vaughan, D.M. (1994) Structure and function of ryanodine receptors. *Am. J. Physiol.*, **266**, C1485–C1504.

Davis, W.L., Hagler, H.K., Farmer, G.R., Martin, J.H. & Bridges, G. (1988) Electron microscopic cytochemical localization of Ca-ATPase in the rod outer segments of the toad Bufo marinus. *Anat. Rec*, **221**, 761–768.

Fain, G.L., Matthews, H.R., Cornwall, M.C. & Koutalos, Y. (2001) Adaptation in vertebrate photoreceptors. *Physiol. Rev.*, **81**, 117–151.

Fessenden, J.D., Feng, W., Pessah, I.N. & Allen, P.D. (2004) Mutational analysis of putative calcium binding motifs within the skeletal ryanodine receptor isoform, RyR1. *J. Biol. Chem.*, **279**, 53028–53035.

Franzini-Armstrong, C. & Jorgensen, A.O. (1994) Structure and development of E-C coupling units in skeletal muscle. *Annu. Rev. Physiol.*, **56**, 509–534.

George, C.H., Rogers, S.A., Bertrand, B.M., Tunwell, R.E., Thomas, N.L., Steele, D.S., Cox, E.V., Pepper, C., Hazeel, C.J., Claycomb, W.C. & Lai, F.A. (2007) Alternative splicing of ryanodine receptors modulates cardiomyocyte Ca^{2+} signaling and susceptibility to apoptosis. *Circ. Res.*, **100**, 874–883.

Giannini, G., Conti, A., Mammarella, S., Scrobogna, M. & Sorrentino, V. (1995) The ryanodine receptor/calcium channel genes are widely and differentially expressed in murine brain and peripheral tissues. *J. Cell Biol.*, **128**, 893–904.

Goldberg, A.F. & Molday, R.S. (2000) Expression and characterization of peripherin/rds-rom-1 complexes and mutants implicated in retinal degenerative diseases. *Meth. Enzymol.*, **316**, 671–687.

Hakamata, Y., Nakai, J., Takeshima, H. & Imoto, K. (1992) Primary structure and distribution of a novel ryanodine receptor/calcium release channel from rabbit brain. *FEBS Lett.*, **312**, 229–235.

Hurley, J.B. & Chen, J. (2001) Evaluation of the contributions of recoverin and GCAPs to rod photoreceptor light adaptation and recovery to the dark state. *Prog. Brain Res.*, **131**, 395–405.

Hurtado, J., Borges, S. & Wilson, M. (2002) Na (+)–Ca (2+) exchanger controls the gain of the Ca (2+) amplifier in the dendrites of amacrine cells. *J. Neurophysiol.*, **88**, 2765–2777.

Kaupp, U.B., Schnetkamp, P.P. & Junge, W. (1981) Rapid calcium release and proton uptake at the disk membrane of isolated cattle rod outer segments. 1. Stoichiometry of light-stimulated calcium release and proton uptake. *Biochemistry*, **20**, 5500–5510.

Kaupp, U.B. & Seifert, R. (2002) Cyclic nucleotide-gated ion channels. *Physiol. Rev.*, **82**, 769–824.

Koulen, P., Kuhn, R., Wassle, H. & Brandstatter, J.H. (1999) Modulation of the intracellular calcium concentration in photoreceptor terminals by a presynaptic metabotropic glutamate receptor. *Proc. Natl Acad. Sci. USA*, **96**, 9909–9914.

Krizaj, D. (2005) Serca isoform expression in the mammalian retina. *Exp. Eye Res.*, **81**, 690–699.

Krizaj, D., Bao, J.X., Schmitz, Y., Witkovsky, P. & Copenhagen, D.R. (1999) Caffeine-sensitive calcium stores regulate synaptic transmission from retinal rod photoreceptors. *J. Neurosci.*, **19**, 7249–7261.

Krizaj, D. & Copenhagen, D.R. (2002) Calcium regulation in photoreceptors. *Front Biosci.*, **7**, d2023–44.

Krizaj, D., Lai, F.A. & Copenhagen, D.R. (2003) Ryanodine stores and calcium regulation in the inner segments of salamander rods and cones. *J. Physiol. (Lond.)*, **547**, 761–774.

Krizaj, D., Liu, X. & Copenhagen, D.R. (2004) Expression of calcium transporters in the retina of the tiger salamander (Ambystoma tigrinum). *J. Comp. Neurol.*, **475**, 463–480.

Laemmli, U.K. (1970) Cleavage of structural proteins during the assembly of the head of bacteriophage T4. *Nature.*, **227**, 680–685.

Lai, F.A., Dent, M., Wickenden, C., Xu, L., Kumari, G., Misra, M., Lee, H.B., Sar, M. & Meissner, G. (1992) Expression of a cardiac Ca (2+)-release channel isoform in mammalian brain. *Biochem. J.*, **288**, 553–564.

Lai, F.A., Misra, M., Xu, L., Smith, H.A. & Meissner, G. (1989) The ryanodine receptor-Ca^{2+} release channel complex of skeletal muscle sarcoplasmic reticulum. Evidence for a cooperatively coupled, negatively charged homotetramer. *J. Biol. Chem.*, **264**, 16776–16785.

Liebman, P.A. (1974) Light-dependent Ca^{++} content of rod outer segment disc membranes. *Invest. Ophthalmol.*, **13**, 700–701.

Liu, D.T., Tibbs, G.R. & Siegelbaum, S.A. (1996) Subunit stoichiometry of cyclic nucleotide-gated channels and effects of subunit order on channel function. *Neuron*, **16**, 983–990.

Lowry, O.H., Rosebrough, N.J., Farr, A.L. & Randall, R.J. (1951) Protein measurement with the Folin phenol reagent. *J. Biol. Chem.*, **193**, 265–275.

Matthews, H.R. & Fain, G.L. (2001) A light-dependent increase in free Ca^{2+} concentration in the salamander rod outer segment. *J. Physiol. (Lond.)*, **532**, 305–321.

McPherson, P.S., Kim, Y.K., Valdivia, H., Knudson, C.M., Takekura, H., Franzini-Armstrong, C., Coronado, R. & Campbell, K.P. (1991) The brain ryanodine receptor: a caffeine-sensitive calcium release channel. *Neuron*, **7**, 17–25.

Meissner, G. (1994) Ryanodine receptor/Ca^{2+} release channels and their regulation by endogenous effectors. *Annu. Rev. Physiol.*, **56**, 485–508.

Molday, R.S. (1998) Photoreceptor membrane proteins, phototransduction, and retinal degenerative diseases. The Friedenwald Lecture. *Invest. Ophthalmol. Vis. Sci.*, **39**, 2491–2513.

Otsu, K., Willard, H.F., Khanna, V.K., Zorzato, F., Green, N.M. & MacLennan, D.H. (1990) Molecular cloning of cDNA encoding the Ca^{2+} release channel (ryanodine receptor) of rabbit cardiac muscle sarcoplasmic reticulum. *J. Biol. Chem.*, **265**, 13472–13483.

Panfoli, I., Morelli, A. & Pepe, I.M. (1994) Characterization of Ca (2+)-ATPase in rod outer segment disk membranes. *Biochem. Biophys. Res. Commun.*, **204**, 813–819.

Panfoli, I., Ravera, S., Fabiano, A., Magrassi, R., Diaspro, A., Morelli, A. & Pepe, I.M. (2007) Localization of the cyclic ADP-ribose-dependent calcium signaling pathway in bovine rod outer segments. *Invest Ophthalmol. Vis. Sci.*, **48**, 978–984.

Panico, J., Parkes, J.H. & Liebman, P.A. (1990) The effect of GDP on rod outer segment G-protein interactions. *J. Biol. Chem.*, **265**, 18922–18927.

Parker, I. & Miledi, R. (1986) Changes in intracellular calcium and in membrane currents evoked by injection of inositol trisphosphate into Xenopus oocytes. *Proc. R. Soc. Lond. B Biol. Sci.*, **228**, 307–315.

Poetsch, A., Molday, L.L. & Molday, R.S. (2001) The cGMP-gated channel and related glutamic acid-rich proteins interact with peripherin-2 at the rim region of rod photoreceptor disc membranes. *J. Biol. Chem.*, **276**, 48009–48016.

van den Pol, A.N. (1988) Silver Intensification of Colloidal Gold or Horseradish Peroxidase for Dual Ultrastructural Immunocytochemistry. Elsevier, Amsterdam.

Saito, A., Seiler, S., Chu, A. & Fleischer, S. (1984) Preparation and morphology of sarcoplasmic reticulum terminal cisternae from rabbit skeletal muscle. *J. Cell Biol.*, **99**, 875–885.

Schnetkamp, P.P. (1995) Calcium homeostasis in vertebrate retinal rod outer segments. *Cell Calcium.*, **18**, 322–330.

Schnetkamp, P.P. & Szerencsei, R.T. (1993) Intracellular Ca^{2+} sequestration and release in intact bovine retinal rod outer segments. Role in inactivation of Na-Ca+K exchange. *J. Biol. Chem.*, **268**, 12449–12457.

Schroder, W.H. & Fain, G.L. (1984) Light-dependent calcium release from photoreceptors measured by laser micro-mass analysis. *Nature.*, **309**, 268–270.

Shoshan-Barmatz, V. & Ashley, R.H. (1998) The structure, function, and cellular regulation of ryanodine-sensitive Ca^{2+} release channels. *Int. Rev. Cytol.*, **183**, 185–270.

Shoshan-Barmatz, V., Hadad-Halfon, N. & Ostersetzer, O. (1995) Cross-linking of the ryanodine receptor/Ca^{2+} release channel from skeletal muscle. *Biochim. Biophys. Acta.*, **1237**, 151–161.

Shoshan-Barmatz, V., Orr, I., Martin, C. & Vardi, N. (2005) Novel ryanodine-binding properties in mammalian retina. *Int. J. Biochem. Cell Biol.*, **37**, 1681–1695.

Shoshan-Barmatz, V., Zalk, R., Gincel, D. & Vardi, N. (2004) Subcellular localization of VDAC in mitochondria and ER in the cerebellum. *Biochim. Biophys. Acta.*, **1657**, 105–114.

Sosa, R., Hoffpauir, B., Rankin, M.L., Bruch, R.C. & Gleason, E.L. (2002) Metabotropic glutamate receptor 5 and calcium signaling in retinal amacrine cells. *J. Neurochem.*, **81**, 973–983.

Suryanarayanan, A. & Slaughter, M.M. (2006) Synaptic transmission mediated by internal calcium stores in rod photoreceptors. *J. Neurosci.*, **26**, 1759–1766.

Takeshima, H., Ikemoto, T., Nishi, M., Nishiyama, N., Shimuta, M., Sugitani, Y., Kuno, J., Saito, I., Saito, H., Endo, M., Iino, M. & Noda, T. (1996) Generation and characterization of mutant mice lacking ryanodine receptor type 3. *J. Biol. Chem.*, **271**, 19649–19652.

Takeshima, H., Nishimura, S., Matsumoto, T., Ishida, H., Kangawa, K., Minamino, N., Matsuo, H., Ueda, M., Hanaoka, M., Hirose, T. & Numa, S. (1989) Primary structure and expression from complementary DNA of skeletal muscle ryanodine receptor. *Nature*, **339**, 439–445.

Towbin, H., Staehelin, T. & Gordon, J. (1979) Electrophoretic transfer of proteins from polyacrylamide gels to nitrocellulose sheets: procedure and some applications. *Proc. Natl Acad. Sci. USA*, **76**, 4350–4354.

Treves, S., Anderson, A.A., Ducreux, S., Divet, A., Bleunven, C., Grasso, C., Paesante, S. & Zorzato, F. (2005) Ryanodine receptor 1 mutations, dysregulation of calcium homeostasis and neuromuscular disorders. *Neuromuscul. Disord.*, **15**, 577–587.

Wang, T.L., Sterling, P. & Vardi, N. (1999) Localization of type I inositol 1,4,5-triphosphate receptor in the outer segments of mammalian cones. *J. Neurosci.*, **19**, 4221–4228.

Yau, K.W. (1994) Phototransduction mechanism in retinal rods and cones. The Friedenwald Lecture. *Invest. Ophthalmol. Vis. Sci.*, **35**, 9–32.

Zarka, A. & Shoshan-Barmatz, V. (1993) Characterization and photoaffinity labeling of the ATP binding site of the ryanodine receptor from skeletal muscle. *Eur. J. Biochem.*, **213**, 147–154.

Zheng, J., Trudeau, M.C. & Zagotta, W.N. (2002) Rod cyclic nucleotide-gated channels have a stoichiometry of three CNGA1 subunits and one CNGB1 subunit. *Neuron*, **36**, 891–896.